A Virtual Confocal Microscope with Variable Diameter to Improve Resolution

Ahmed M. D. E. Hassanein
Systems and Information Department, Engineering Division,
National Research Centre (NRC), Dokki, Giza,
Egypt
Email: ahmed22@aucegypt.edu

Abstract—**A widely known process to examine malign tissues is microwave imaging. It depends on the contrast in dielectric properties between malign and benign tissues. The virtual confocal microscope is one of the methods which uses microwave frequencies to detect cancer. It focuses the incoming reflected waves from the tissues using a virtual lens to form a cross sectional image of the object being imaged. Here, we highlight a mathematical relationship that relates the distance between the virtual lens and the obtained image with specific values for the diameter of the virtual lens used. The allowed diameters of the lens for a given specific distance from lens to image are calculated. Two objects are proposed to be used to clarify the idea. One object stands at the center of the virtual lens and the other is placed off the center. For each object, two images are calculated and compared. One image is calculated using a random value for the diameter of the lens. Another image is calculated using one of the allowed diameters for the virtual lens. The images which are calculated using the allowed diameter have proven to be of a better quality even when objects are placed off the center.**

Keywords—Confocal Imaging; Lens Design; Microwave Frequency; Resolution; Virtual Microscope

I. INTRODUCTION

Cancer detection is one of the leading topics due to the benefits which can be gained in curing people. Cross sectional imaging is gaining a lot of interest in recent research work as a tool to diagnose malign tissues as early as possible and so increase the probabilities of curing people. The imaging process depends on several issues such as the electrical properties of tissues being imaged, the bandwidth which is used in imaging, and the reconstruction techniques of the received signals from the tissues. Each of these topics has gained a lot of research interest as to be discussed in this section.

Among the various breast imaging modalities for breast cancer detection, microwave imaging is important due to the high contrast in dielectric properties between healthy and malign tissues [1]. The microwave bandwidth is defined in the range from 3.1 to 10.6 GHz [1]. The knowledge of these properties at the microwave frequencies has been limited due to lack of complete information in the reported small-scale studies [2]. Due to those reasons, this modality has received a significant interest and attention from the microwave community [1]. Lazebnik et al. characterize the wideband microwave-frequency dielectric properties for a large number of samples of normal breast tissue which are obtained from different surgeries at the hospitals of University of Wisconsin and University of Calgary [2].

In Confocal microwave imaging, a breast is illuminated with a pulse of ultra-wideband wave from a number of antenna locations. Then, the captured reflections from the breast are synthetically focused [3] [4]. In ref [3], the detection of malign tissues is achieved by the coherent addition of the returns from strongly scattering objects. The success of detecting and localizing small tumors in three dimensions with numerical models of two system configurations involving synthetic cylindrical and planar antenna arrays are demonstrated in [3]. In ref [4], detection of tumors within the breast is achieved by some selected focusing technique. Image formation algorithms are designed to differentiate between tumor responses and early-time and late-time clutter which are reflected from skin and normal tissues with different dielectric properties [4]. Jacobsen et al. evaluate the performance of the cross-correlated back projection imaging scheme by using a scanning system in phantom experiments. The phantom is scanned with a synthetic broadband elliptical antenna in a mono-static configuration [4].

In microwave imaging, the body being imaged is scanned using microwave frequencies and the backscattered signal is in the microwave range of frequencies as well. Another way for imaging biological tissue is thermoacoustic imaging. In it, a body is radiated with multiple microwave radiation pulses [5]. The microwave pulses are swept across a range of microwave frequencies [5]. In response, the tissue region backscatters multiple thermoacoustic signals which are detected through specially tailored antennas for this cause [5].

Another way to examine human cells is the emerging optoacoustic imaging one [6]. Optoacoustic imaging includes features which are required in an ideal method such as high contrast and versatility in sensing different tissues, excellent spatial resolution, and relatively low cost of implementation [6]. The

transmitted signal is in the microwave frequencies but the response of the tissues is an optoacoustic pulse. Lutzweiler et al. discuss the advantages and disadvantages of some of the available optoacoustic image reconstruction and quantification approaches such as back-projection and model-based inversion algorithms, sparse signal representation, wavelet-based approaches, methods for reduction of acoustic artifacts and multi-spectral methods for visualization of tissue bio-markers [6].

In ref [7], a confocal microwave imaging system for the detection of early-stage breast cancer is discussed. A microwave sensor is proposed which presents a novel adaptation and application of the principles of ultra wideband radar technology and confocal optical microscopy [7]. The sensor is comprised of an electronically switched monostatic antenna array that synthetically focuses a low-power pulsed microwave signal at a focal point within the breast and collects the backscattered signal [7]. High quality ultra wide-band measurements provide a basis for understanding the transient scattering phenomena necessary for the development of short-pulse radar target identification and detection schemes [8].

An image reconstruction algorithm is presented in [9] which is computationally efficient and robust for breast cancer detection using an ultra-wideband confocal microwave imaging system. The image reconstruction algorithm is applied to FDTD-computed backscatter signals, resulting in a microwave image that clearly identifies the presence and location of the malignant lesion [9].

In ref [10], a reconstruction algorithm for imaging large tissue areas with microscopic resolution in vivo is presented. Spectrally encoded confocal microscopy is proposed as an approach for performing confocal imaging. A unique probe configuration and scanning geometry are used which gives the advantages of having a speed and resolution sufficient for comprehensively imaging large tissues areas at a microscopic scale in times that are appropriate for clinical use [10].

Microscopes have been traditionally designed to use the human eye to observe the image [11]. But, nowadays digital cameras are used as the imaging device in both standard and confocal microscopes. These new digital detectors are more sensitive to intensity and flatness differences than the human eye and require new strategies for objective lens design [11]. Many modern microscope objectives are well suited for confocal scanning as long as they are used within their design specifications [12] [13]. With the ever-wider use of confocal scanning microscopy for 3D live-cell imaging and with new microscope techniques emerging, new and improved objectives continue to appear [12] [13].

A lens is an optical element with two surfaces, at least one of which is curved. Lenses of many different shapes and sizes are ubiquitous in optical systems as diverse as animal eyes, cameras or laser systems [14].

The light gathering and focusing properties of lenses are well described by geometrical optics and optimization of lens geometry to provide the best performance is traditionally done using the laws of geometrical optics [14]. However, physical optics, which describes the propagation of light waves through space, must be used to obtain detailed understanding of the focusing behavior of lenses [14].

In this paper, we study if changing the diameter of the lens for a virtual confocal microscope can help us to obtain a perfect image for a certain target object. In section 2, the idea of the virtual confocal microscope is explained so as to be adapted to the objective of this paper. The theoretical background which is used to define some allowed values for the diameter of the lens is laid out. In section 3, the calculated results are shown and illustrated. Two examples of imaging are shown so as to clarify the difference in the quality of images when using the allowed values. In section 4, a discussion of the results is explained and conclusions are drawn finally.

II. METHODOLOGY AND THEORETICAL FOUNDATION

In this section, we describe the confocal imaging system which we would like to improve. The new in this paper is the way through which already mentioned theory available in the research papers is viewed and described. In one subsection, the system by which the confocal imaging method works and the proposed modification are explained. In another subsection, the equations and mathematical foundations for the proposed solution are described.

A. Confocal Imaging System

The virtual confocal microscope is composed of two steps [15]. The first is applied inside the experimental laboratory and is shown in fig 1. An object which emits a wave front is placed at a distance z_1 from an array of antennas. An example of a receiver antenna (Rx) is shown. For an object, a synthetic wave front is constructed using an array of point sources. The Point sources have uniform amplitude equal to one and they are phase locked together and placed along a line on the ξ axis as shown. The object is used to generate a test wave front which is what we can capture by the array of antennas. The length of the array of antennas forms the angle of view by which the object is imaged. In the second step, the test wave front is computationally passed through a virtual thin lens (not shown in figure). The lens has the same diameter as the length of the array of antennas. By varying the intermediate distance (shown in fig 1) between the arrays of antennas, the diameter of the virtual lens can be varied. The lens focuses computationally the incoming wave front to form an image at the far side of the lens from the object. An image is calculated using monochromatic signal.
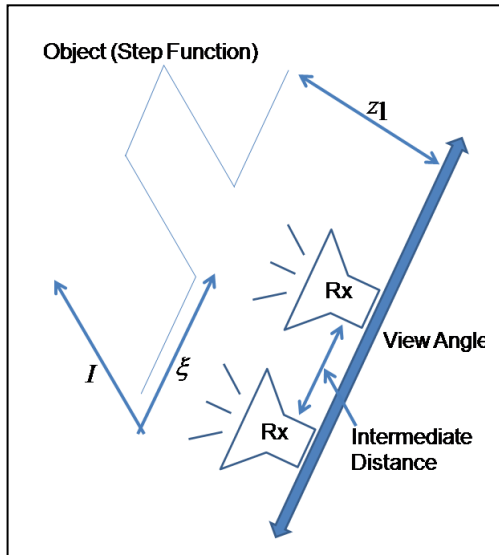
Fig. 1.: *A sketch shows how a virtual confocal microscope can work with a lens of variable diameter.*

B. Imaging Equations

The relation between an object behind a lens and its image in front of the lens can be seen as a convolution. The propagation from an object plane $U_O(\xi,\eta)$ to an image plane $U_i(u,v)$ through a thin lens can be described as follows [16]:

$$U_i(u,v) = \int\limits_{-\infty}^{\infty}\!\!\int U_O(\xi,\eta)h(u,v;\xi,\eta)d\xi d\eta \qquad (1)$$

where the impulse function $h(u,v;\xi,\eta)$ describes the imaging system in the confocal imaging technique. Here, we use the one dimensional form of eq (1) which can be expanded to two dimensional form in future work. Towards this aim, we redefine the object as follows [15]:

$$U_O(\xi,\eta) = U_O(\xi,\eta)\delta(\eta) \qquad (2)$$

where $\delta(\eta)$ is a delta function.

$$U_i(u,v) = \int\limits_{-\infty}^{\infty}\!\!\int U_O(\xi,\eta)\delta(\eta)h(u,v;\xi,\eta)d\xi d\eta \qquad (3)$$

$$U_i(u,v) = \int\limits_{-\infty}^{\infty} U_O(\xi,\eta=0)h(u,v;\xi,\eta=0)d\eta \qquad (4)$$

$$U_i(u,v=0) = \int\limits_{-\infty}^{\infty} U_O(\xi,\eta=0)h(u,v=0;\xi,\eta=0)d\eta$$

The intensity of the obtained image is:

$$I = |U_i(u,v=0)|^2 \qquad (5)$$

Using the Huygen's Fresnel principle, the function $h(u,v=0;\xi,\eta=0)$ takes the following form [16]:

$$h(u,v=0;\xi,\eta=0) = \frac{1}{\lambda^2 z_1 z_2}\int \exp\left\{\frac{-j2\pi}{\lambda z_2}[(u-M\xi)x]\right\}dx \qquad (6)$$

where λ is the wavelength, z_1 is the distance from object to lens, z_2 is the distance from lens to image, ξ is the object axis, u is the image axis, x is the lens axis and M is the magnification of the lens used.

The relationship between z_1 and z_2 is [16]:

$$\frac{1}{f} = \frac{1}{z_1} + \frac{1}{z_2}$$

where f is the focal length of the lens.

The exponential part in the 1-D solution (eq (6)) can take the form:

$$\exp\left\{\frac{-j2\pi}{\lambda z_2}(u-M\xi)x\right\} = \cos\left[\frac{2\pi}{\lambda z_2}(u-M\xi)x\right] + j\sin\left[\frac{2\pi}{\lambda z_2}(u-M\xi)x\right] \qquad (7)$$

The object being imaged starts with an amplitude equal one and phase equal zero. In order to obtain a replica of the object, we need to maximize the real part of eq (7). Taking the real part only of eq (7), we get:

$$\cos\left[\frac{2\pi}{\lambda z_2}(u-M\xi)x\right] \qquad (8)$$

when this term is maximum, we get maximum resolution in our image.

In other words, we need to make:

$$\cos\left[\frac{2\pi}{\lambda z_2}(u-M\xi)x\right] = 1 \qquad (9)$$

then

$$\left[\frac{2\pi}{\lambda z_2}(u-M\xi)x\right] = 2n\pi \qquad (10)$$

where $n = 0,1,2,3,4,\ldots\ldots$

Then the lens diameter x can be expressed in the following form:

$$x = \frac{n\lambda z_2}{(u-M\xi)} \qquad (11)$$

where $M = \dfrac{z_2}{z_1}$.

III. RESULTS

In this section, Matlab^{TM} is initiated to be used to calculate eq (5) and (11). The allowed values for the diameter of the virtual lens which is required to calculate a perfect image are calculated. An object similar to that shown in fig 1 is used to test the

possible diameters of the lens in forming an image. The intensity "I" for the side lobes and the center point of an image are the two parameters which are used to evaluate our results. Two cases are studied in this section. In one case, we use an object which is placed at the center of the object space (ξ, η). In another case, an object which is placed off the center of the object space is used.

A. Variable Diameter

In this subsection, eq (11) is used to calculate the possible values for the diameter of the virtual lens. Those values enable us to calculate the best possible image for the object being imaged. The wavelength which is used in our calculations is $\lambda = 0.006$ m. The distance between the lens and the calculated image which is used is $z_2 = 0.2$ m. The amplification ratio for the lens which is used is $M = 1$. When $(u - \xi)$ have the smallest value other than zero, we can get the possible values of the lens diameter x. The minimum difference between the pixels in the object space and that in the image space is $(u - \xi)_{\min} = 0.002$ m.

Using the above mentioned values in eq (11), the possible values for the diameter of the lens can be calculated as shown in table I.

TABLE I.   : A SERIES OF DIFFERENT DIAMETERS AT WHICH IMAGES WITH BETTER RESOLUTION CAN BE CALCULATED.

n	Lens Diameter (x)
1	0.59
2	1.2
3	1.78
4	2.38
5	2.97

Each diameter which is shown in table I corresponds to a different value for the parameter n. The diameter of the virtual lens for $n = 0$ is omitted because it is a non-practical value.

By examining the equation:

$$\frac{x}{z_2} = \frac{n\lambda}{(u - M\xi)}$$

The right hand side of this equation is constant and the whole equation is independent of z_1.

So if I have several objects each one corresponds to a different z_1 that is to say: z_{10}, z_{11}, z_{12}, z_{13},

Each of these z_1 corresponds to a different z_2 namely z_{20}, z_{21}, z_{22}, z_{23}, ………. So, if we need a specific z_2 then we need to calculate the corresponding x (lens diameter) that would keep the ratio on the left hand side the same where x_0 corresponds to z_{20}, x_1 corresponds to z_{21}, and so on.

B. Better Imaging Resolution

In this subsection, eq (5) is used to calculate images for different objects used. Two objects are set to test the possible calculated values for the diameters of the lens. For each case, an image is calculated for the object used using two values of the diameters. One value is taken from table I which is calculated using eq (11). We have chosen the value which is calculated for $n = 1$. A second value is chosen randomly for the diameter of the lens to calculate the image of the object. The second choice is used to clarify the difference when choosing a diameter different than the proposed ones in table I.
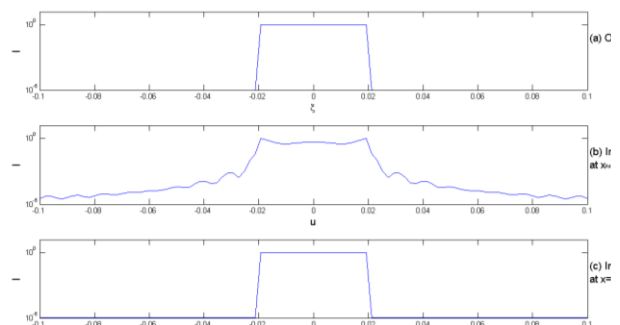

Fig. 2.*: The object and its images at two different diameters of the virtual lens used. (a) shows a line of point sources placed at center of object space. (b) shows an image of the object when x is approximately 1m. (c) shows an image of the object when x is equal 0.59m.*

The object in fig 2a is composed of 100 pixels with a total length of 0.2m. It contains an array of point sources which have amplitude equal to one and a total length equal 0.05m. The starting phase of all point sources is zero. They are placed so that the center of the array is at the point $\xi = 0$ m. Eq (5) is used to calculate the image of the object after propagating through a thin lens. The image when using a diameter of lens approximately equal to 1m is shown in fig 2b. Another image which is calculated when using a diameter of lens approximately equal to 0.59m is shown in fig 2c. The results which are seen in fig 2 are tabulated in table II.

TABLE II.   : THE RESULTS IN FIG 2 ARE TABULATED.

$x \setminus u$	0	0.04
1	0.5344	0.0005377
0.59	0.9999	0.00001

In fig 2b, the intensity of the image at $u = 0$ is 0.5344. While, the intensity of the image at the side lobe $u = 0.04$ is 0.0005377. The image doesn't represent the object being imaged. The same calculations are repeated but while using the defined diameter at $n = 1$. In fig 2c, the intensity of the image at $u = 0$ is 0.9999. While, the intensity of the image at the side lobe $u = 0.04$ is 0.00001. The intensity for the side lobe has decreased to 1/50 of the value in fig 2b. The image in fig 2c is a good representation of the object being imaged. The closer the imaged object to the central axis of the virtual lens, the more balanced is

the emitted waves which are collected by the lens from both sides of that object and so the better the ability of the lens to form an accurate image of the object. Next, the position of the object is changed to test imaging objects which are placed away from the central axis of the virtual lens.
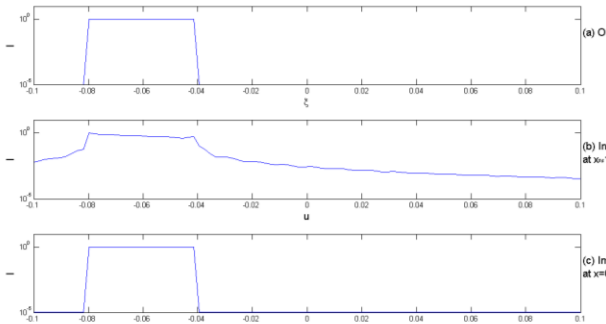

Fig. 3.: *(a) shows a line of point sources placed at the left side of object space. (b) shows image when x is approximately 1m. (c) shows image when x is equal 0.59m.*

The object in fig 3a has the same properties as that which is shown in fig 2a. But, the only difference is that the center of the array of point sources has moved so that it is placed at the point $\xi = 0.06$ m. Eq (5) is again used to calculate the image of the object after propagating through a thin lens. The two images which are shown in fig 3b and 3c are calculated using the same diameters of lens as those used in fig 2b and 2c respectively. The results which are seen in fig 3 are tabulated in table III.

TABLE III. : The results in fig 3 are tabulated.

$x \setminus u$	0.06	0.1
1	0.611	0.00628
0.59	0.9973	0.000011

In fig 3b, the intensity of the image at $u = 0.06$ is 0.611. While, the intensity of the image at the side lobe $u = 0.1$ is 0.00628. The intensity value of the side lobe has increased than that shown in fig 2b because the object is placed off the center. The image doesn't represent the object being imaged. The same calculations are repeated but while using the defined diameter at $n = 1$. In fig 3c, the intensity of the image at $u = 0.06$ is 0.9973. While, the intensity of the image at the side lobe $u = 0.1$ is 0.000011. The image in fig 3c is a good representation of the object being imaged even when it is moved away from the center of the lens.

IV. DISCUSSION AND CONCLUSION

Breast cancer detection has gained a wide interest in the research community. One of the most successful techniques to detect malign tissues is microwave imaging because it depends on the contrast in dielectric properties between malign and benign tissues. The virtual confocal microscope method uses microwave frequencies to detect cancer. In this paper, we propose modifying the view angle of the virtual lens which is used in the method so as to improve the

resolution of the obtained images. A mathematical relationship is found that relates the values of the diameter of the virtual lens to the distance between the lens and the image plane. The possible allowed values for the diameter of the lens are tabulated to image a proposed one dimensional object. An array of point sources with amplitude equal to one is placed at the center of the object plane to test the validity of the proposed modification. The image which is calculated using a random value for the diameter of the virtual lens doesn't represent the object due to the presence of side lobes. But, the proposed calculated values for the diameter improved the quality of the obtained images significantly. It is generally known that the wider the diameter of the lens the more scattered waves which can be collected by the lens from the object and so the better the ability of the lens to form an accurate image for the object [15]. Although the random diameter is larger than the proposed one, still the image calculated using the later one is better than that calculated using the earlier one. The center of the array of point sources is moved to be on the left hand side of the object plane. The image which is calculated using the random diameter has even deteriorated due to the fact that the object is placed off the center of the virtual lens. But, the calculated diameter has again improved the quality of the obtained images. The proposed modification has proved to be a success in improving the resolution of the obtained images. Improving the quality of images in cancer detection helps in increasing the probability of detecting cancer in its early stages and so increasing the chances of curing it.

REFERENCES

[1] Zhurbenko, V. "Challenges in the Design of Microwave Imaging Systems for Breast Cancer Detection." Advances in Electrical and Computer Engineering 11.1 (2011): 91-96.

[2] Lazebnik, Mariya, Leah Mccartney, Dijana Popovic, Cynthia B. Watkins, Mary J. Lindstrom, Josephine Harter, Sarah Sewall, Anthony Magliocco, John H. Booske, Michal Okoniewski, and Susan C. Hagness. "A Large-scale Study of the Ultrawideband Microwave Dielectric Properties of Normal Breast Tissue Obtained from Reduction Surgeries." Physics in Medicine and Biology 52.10 (2007): 2637-656.

[3] Fear, E. C., X. Li, S. C. Hagness, and M. A. Stuchly. "Confocal Microwave Imaging for Breast Cancer Detection: Localization of Tumors in Three Dimensions." IEEE Transactions on Biomedical Engineering 49.8 (2002): 812-22.

[4] Jacobsen, S., and Y. Birkelund. "Improved Resolution and Reduced Clutter in Ultra-Wideband Microwave Imaging Using Cross-Correlated Back Projection: Experimental and Numerical Results." International Journal of Biomedical Imaging 2010 (2010): 1-10.

[5] Li, Jian, and Gang Wang. Multi-Frequency Microwave-Induced Thermoacoustic Imaging Of

Biological Tissue. University of Florida Research Foundation, Inc., Gainesville, FL (US), assignee. Patent US 7,266,407 B2. 04 Sept. 2007.

[6] Lutzweiler, Christian, and Daniel Razansky. "Optoacoustic Imaging and Tomography: Reconstruction Approaches and Outstanding Challenges in Image Performance and Quantification." Sensors 13.6 (2013): 7345-384.

[7] Hagness, S. C., A. Taflove, and J. E. Bridges. "Three-dimensional FDTD Analysis of an Ultrawideband Antenna-array Element for Confocal Microwave Imaging of Nonpalpable Breast Tumors." Antennas and Propagation Society International Symposium. Proc. of IEEE. Vol. 3. : 1999. 1886-889. Print. doi: 10.1109/APS.1999.788325

[8] Rothwell, Edward J., Kun M. Chen, Dennis P. Nyquist, John Ross, and Robert Bebermeyer. "Measurement and Processing of Scattered Ultrawideband/short-pulse Signals." Proc. SPIE 2562. Vol. 138: 1995. Print. Radar/Ladar Processing and Applications. http://dx.doi.org/10.1117/12.216950

[9] Li, Xu, and S.c. Hagness. "A Confocal Microwave Imaging Algorithm for Breast Cancer Detection." IEEE Microwave and Wireless Components Letters 11.3 (2001): 130-32.

[10] Yelin, D., C. Boudoux, B. E. Bouma, and G. J. Tearney. "Large Area Confocal Microscopy." Optics Letters 32.9 (2007): 1102.

[11] Drent, Peter. "Properties and Selection of Objective Lenses for Light Microscopy Applications." Microscopy and Analysis 19.6 (2005): 5-7. Nikon Instruments Europe. John Wiley & Sons, Ltd.

[12] Keller, H. E. "Objective Lenses for Confocal Microscopy." Handbook of Biological Confocal Microscopy. Ed. James B. Pawley. Third ed. New York, NY: Springer, 2005.

[13] Dobson, Sarah L., Pang-Chen Sun, and Yeshayahu Fainman. "Diffractive Lenses for Chromatic Confocal Imaging." Applied Optics 36.20 (1997): 4744.

[14] Guha, Shekhar, Leonel P. Gonzalez, and Qin Sheng. "Description of Light Focusing by a Spherical Lens Using Diffraction Integral Method." PAMM. Proc. Appl. Math. Mech. 7. : Print. DOI 10.1002/pamm.200700051.

[15] Hassanein, A D, Imaging Techniques Using Ultra Wide Band, PhD Thesis, University of Oxford, 2009.

[16] Goodman, J W, Introduction to Fourier Optics, NewYork, McGraw-Hill, 1996.